Cathodic Materials

Deutsche Ausgabe: DOI: 10.1002/ange.201600661
Internationale Ausgabe: DOI: 10.1002/anie.201600661

Synthesis of Monocrystalline Nanoframes of Prussian Blue Analogues by Controlled Preferential Etching

Wei Zhang, Yanyi Zhao, Victor Malgras, Qingmin Ji, Dongmei Jiang, Ruijuan Qi, Katsuhiko Ariga, Yusuke Yamauchi, Jian Liu, Ji-Sen Jiang,* and Ming Hu**

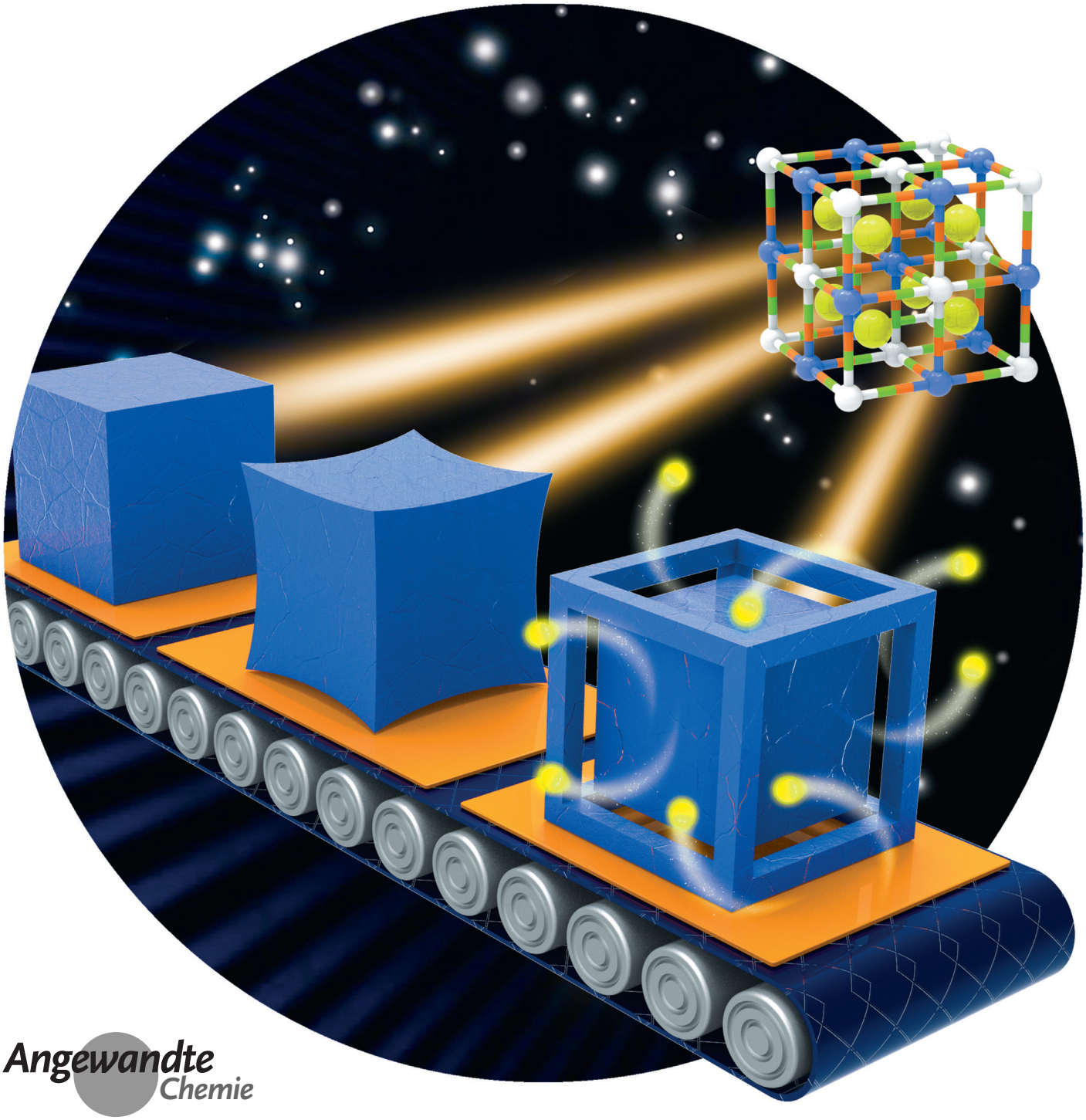

Abstract: *Metal cyanide coordination compounds are recognized as promising candidates for broad applications because of their tailorable and adjustable frameworks. Developing the nanostructure of a coordination compound may be an effective way to enhance the performance of that material in application-based roles. A controllable preferential etching method is described for synthesis of monocrystalline Prussian blue analogue (PBA) nanoframes, without the use of organic additives. The PBA nanoframes show remarkable rate performance and cycling stability for sodium/lithium ion insertion/extraction.*

Coordination compounds, such as transition metal ions linked by short ligands (cyanides for example), metal–organic frameworks (MOFs), or porous coordination polymers (PCPs), are an emerging class of functional solids with open pores.[1] The tailorable/adjustable nature of coordination frameworks render these materials promising for applications in electric energy storage (EES) or catalysis, among others.[2–4] The performance of coordination compounds in such applications strongly depends on structural features,[4,5] and the synthesis of nanostructures with combined structural advantages (high crystallinity and a large contactable surface area, for example) are of interest.

Monocrystalline nanoframes, a class of hollow nanostructures with holes on each face, are ideal candidates because they can simultaneously offer high-crystallinity and a large contactable surface area.[6] Coordination compounds with a monocrystalline frame-like nanostructure are expected to be promising candidates for EES applications. However, it remains challenging to fabricate such nanostructures. Several attempts have been made to fabricate hollow-based coordination compounds.[7–9] Unfortunately, none of these efforts have led to the synthesis of monocrystalline nanoframes. Therefore, new methods for fabrication of monocrystalline coordination compound nanoframes are vital.

Herein, we describe a novel nanostructured coordination compound prepared by organic-free preferential etching. Etching has been widely applied in nanostructuring of amorphous silica, noble metals, or semiconductors.[6,10] Recently, polymeric additives or organic acids have shown promising results in controlling the etching of coordination compounds.[11] However, organic molecules can be trapped inside pores, leading to blockage. Thus, organic additives are unfavorable in EES applications. Unfortunately, organic-free etching methods are poorly developed because of limited knowledge about the etching kinetics of coordination compounds in acidic or basic media.[11] To selectively etch coordination compounds in such media, different etching kinetics should be utilized when dealing with specific structural features. Controlled etching may be susceptible to the location at which the process takes place; on corners, edges, or faces.[12] In principle, monocrystalline coordination compounds nanoframes can be obtained with the aid of selective etching.

The coordination compound investigated herein is a Prussian blue analogue (PBA, $A_xM[M'(CN)_6]_y\cdot\square_{1-y}\cdot nH_2O$: A = alkali metal; M,M′ = transition metals; □ = M′(CN) vacancy; $0 \le x \le 2$; $0 < y \le 1$). PBAs are recognized as promising materials because of their redox active metal ions and open zeolite-like frameworks.[13] The fabrication of nanoframe structures is achieved by applying a preferential etching process to pre-formed crystals, as shown in Figure 1. Monocrystalline $Na_{1.76}Ni[Fe(CN)_6]_{0.94}$ (NiFe(II)) PBA is synthesized by a kinetically controlled crystallization method, as shown in Figure 1 a-1, 1 a-2, and Figure S1 a (Supporting Information).[14] The initial PBA crystals possess a cubic shape with a size of about 200–400 nm. The electron diffraction (ED) pattern obtained from an isolated single-crystal was typical of PBA (insets of Figure 1 a-2). The NiFe(II) PBA cubes were subsequently incubated in a HCl solution under ambient conditions to generate NiFe(II) PBA nanoframes. Samples harvested at different stages of the reaction (0, 5, and 60 min) were examined to trace the evolution of the morphology, as well as crystal structure and composition (Figure 1 a–c). During the first 5 min, the size of the cubes did not change significantly. However, bright edges are an indication of slight etching on each face. Figure S1 b (Supporting Information) further confirms that the faces of the cubes are etched, leading to the formation of concave shapes. The concave cubes exhibited a similar single-crystal-like ED behavior compared to the initial cubes. The squared ED pattern is displayed in the inset of Figure 1 b-2, which is the same as the ED pattern of the cubes, indicating that concave cubes possess a crystal structure that is similar to that of the initial cubes. After 1 h, nanoframe-like structures were observed, as shown in Figure 1 c-2. The overall size of the nanoframes was similar to that of the initial cubes. The external faces were almost entirely dissolved, leaving the skeletons with a diameter of around 50 nm. Interestingly, the skeletons retained a monocrystalline structure. The periodic ED spots on a whole nanoframe indicate highly orientated nanoframes (the inset of Figure 1 c-2).

The nanoframes exhibit a different crystal structure compared to the initial cubes and intermediate concave cubes. The pure rhombohedral structure found in the initial cubes and the intermediate concave cubes transformed into a face-centered-cubic (*fcc*) structure in the final nanoframes,

[*] W. Zhang, Y. Zhao, Prof. Dr. D. Jiang, Prof. Dr. J.-S. Jiang, Dr. M. Hu
School of Physics and Materials Science, East China Normal University, Shanghai, 200241 (China)
E-mail: jsjiang@phy.ecnu.edu.cn
mhu@phy.ecnu.edu.cn
Dr. V. Malgras, Prof. Dr. K. Ariga, Prof. Dr. Y. Yamauchi
International Center for Materials Nanoarchitectonics (MANA), National Institute for Materials Science (NIMS), Tsukuba (Japan)
Prof. Dr. Q. Ji
Herbert Gleiter Institute of Nanoscience, Nanjing University of Science and Technology, Nanjing (China)
R. Qi
Key Laboratory of Polar Materials and Devices, East China Normal University, Shanghai, 200262 (China)
Dr. J. Liu
Department of Chemical Engineering, Curtin University
Perth, WA 6845 (Australia)
E-mail: jian.liu@curtin.edu.au

Supporting information for this article can be found under: http://dx.doi.org/10.1002/anie.201600661.

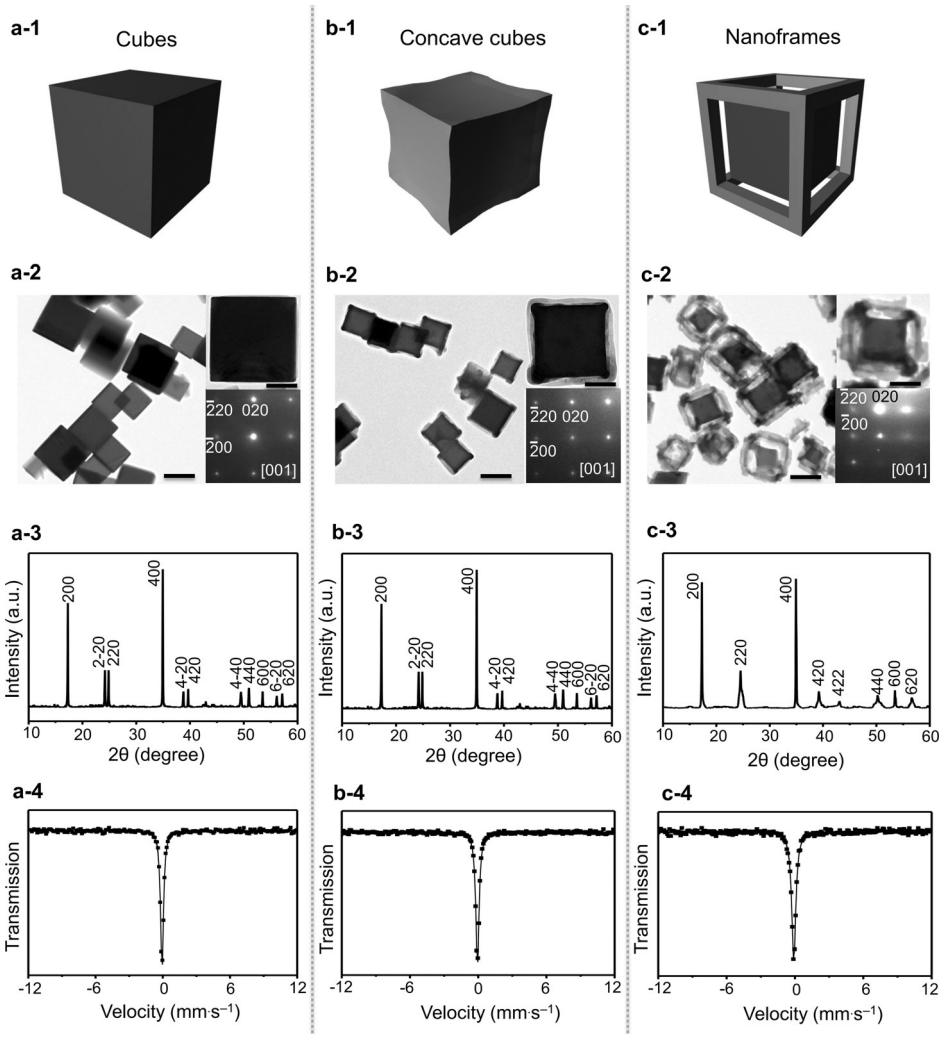

Figure 1. Nanostructure evolution: a-1) NiFe(II) PBA cubes, b-1) NiFe(II) PBA concave cubes, and c-1) NiFe(II) PBA nanoframes. TEM images of: a-2) NiFe(II) PBA cubes, b-2) NiFe(II) PBA concave cubes, and c-2) NiFe(II) PBA nanoframes. Scale bars: left (100 nm), middle (200 nm), right (100 nm), and inset images (50 nm). Wide-angle XRD patterns of: a-3) NiFe(II) PBA cubes, b-3) NiFe(II) PBA concave cubes, and c-3) NiFe(II) PBA nanoframes. Mössbauer spectra of: a-4) NiFe(II) PBA cubes, b-4) NiFe(II) PBA concave cubes, and c-4) NiFe(II) PBA nanoframes.

according to the powder X-ray diffraction (PXRD) profiles (Figures 1 a-3, 1 b-3, and 1 c-3). Atomic composition varied slightly during the etching process. The Fe:Ni ratios changed from 0.94 (initial cubes) to 0.92 (concave cubes), and finally to 0.8 (nanoframes), suggesting disassembly of $[Fe(CN)_6]^{4-}$ complexes from the framework. On the other hand, Mössbauer spectra reveal that the bulk valence of iron during the etching process remains +2, which is attributed to a singlet derived from low spin Fe^{2+}. On the basis of the above results, it can be stated that the initial NiFe(II) PBA cubes are gradually etched and converted into NiFe(II) PBA concave cubes in the first stage, and finally into NiFe(II) PBA nanoframes (with an Fe:Ni ratio of 0.8).

The evolution of nanostructure by preferential etching is discussed further below. In brief, HCl is able to break the coordination bonds within the PBA framework to generate Ni^{2+} and $[Fe(CN)_6]^{4-}$ ions, as confirmed by UV/Vis spectroscopy (Supporting Information, Figure S2). This reaction only requires labile protons provided by HCl. For instance, an equivalent concentration of acetic acid did not etch the PBA (Supporting Information, Figure S3). However, nanoframes can be obtained in the presence of HCl without other possible reactants (oxygen for example) dissolved in water (Supporting Information, Figure S4). It is known that disordered domains or defects manifest heterogeneously inside MOF or coordination polymer crystals (even single-crystals).[12a] Defects such as the dangling bonds of ligands, amorphous parts, and polycrystalline domains, can easily be generated during a non-classical crystallization process.[9a] The heterogeneously distributed defects inside MOF crystals can induce non-uniform etching kinetics, depending on the local concentration of defects.[12] For example, the etching rate can be faster in regions with more defects. It was previously reported that the flat surfaces of PBAs are of a lower stability than the corners or the edges.[15] Thus, the middle of the external faces of the cubes can be dissolved faster during the etching process, leading to a nanoframe-like morphology.

To confirm that the etching process starts from the surface, changes to the surface were investigated by X-ray photoelectron spectroscopy (XPS; Supporting Information, Figure S5). The valence of iron at the surface of the cubes was +2,[13c,16] and no oxidation was detected. The presence of a partially oxidized iron on the surface of the concave cubes is supported by the extra doublet located at 710.5 eV and 723.1 eV, which can be assigned to $Fe^{III}2p_{3/2}$ and $Fe^{III}2p_{1/2}$, respectively.[13c,16] The content of Fe^{III} on the surface increased slightly after the formation of nanoframes, indicating that more surface Fe^{II} was oxidized into Fe^{III}. Generation of Fe^{III} on the surface during the etching process was further confirmed by Raman and Fourier transform infrared spectroscopy (FT-IR; Supporting Information, Figures S6–S7). Compared with the Raman spectrum of the initial cubes, the concave cubes and the nanoframes present an extra peak at 2177 cm^{-1}, which represents Fe^{III}-CN-Ni^{II} (Supporting Information, Figure S6).[17] A new peak centered at 2163 cm^{-1}, which corresponds to CN coordinated by Ni^{II} and Fe^{III}, was also observed in the FT-IR profiles of the concave cubes and nanoframes (Supporting Information,

Figure S7).[18] Notably, generation of Fe^{III} was not detected in the Mössbauer spectra (operating on transmission mode), giving an over-arching perspective of the iron valence inside the whole sample. Thus, the generation of Fe^{III} detected by XPS suggests that oxidation of Fe^{II} only takes place on the surface, which supports the idea that the etching preferentially occurs in the middle of the surfaces of the PBA cubes. Oxidation of the surface is probably a result of the high reactivity of the freshly exposed surface of the PBA. The high activity of the surface allows the O_2 dissolved in water to oxidize the Fe^{II}. Previous reports have already demonstrated that doping of PBA frameworks with Fe^{III} leads to an *fcc* structure rather than a rhombohedral structure.[19] Thus, the generated Fe^{III} on the surface probably guides transformation of the crystal structure from rhombohedral to *fcc*.

The specific surface areas of the NiFe(II) PBA nanoframes were measured by nitrogen adsorption–desorption analysis at 77 K (Supporting Information, Figure S8). The specific surface areas were calculated by the Brunauer–Emmett–Teller (BET) method. The nanoframes have a BET surface area of $30\ m^2 g^{-1}$, which is consistent with the formation of nanosized skeletons.

As a typical EES application, we selected a sodium ion (Na^+) battery test. The sodium ion battery is recognized as an economical alternative to high-cost lithium ion batteries for large-scale EES applications.[20] The small internal spacing of common battery materials, such as the spinel metal oxides employed in conjunction with lithium ion batteries, cannot accommodate the large radius of Na^+ ions (1.02 Å). In contrast, PBA materials with open frameworks, have great potential.[13] Significant enhancement of the electrochemical performance of the nanoframes was found in a PBA/Na half-cell test. Although the initial cyclic voltammetry (CV) curves and galvanostatic charge/discharge cycling curves of the nanoframes are similar to the initial PBA cubes (Supporting Information, Figure S9), the rate performance and cycling stability of the nanoframes are much better than that of the PBA cubes. The NiFe(II) PBA nanoframes present an excellent rate performance, as shown in Figure 2a. When the charge/discharge current rate was as high as $1000\ mA g^{-1}$, the nanoframes showed a capacity retention ratio as high as 61%, whereas the initial cubes could only retain 17% of the initial capacity. After 500 cycles, the nanoframes retained 90% of their initial capacity (Fig-

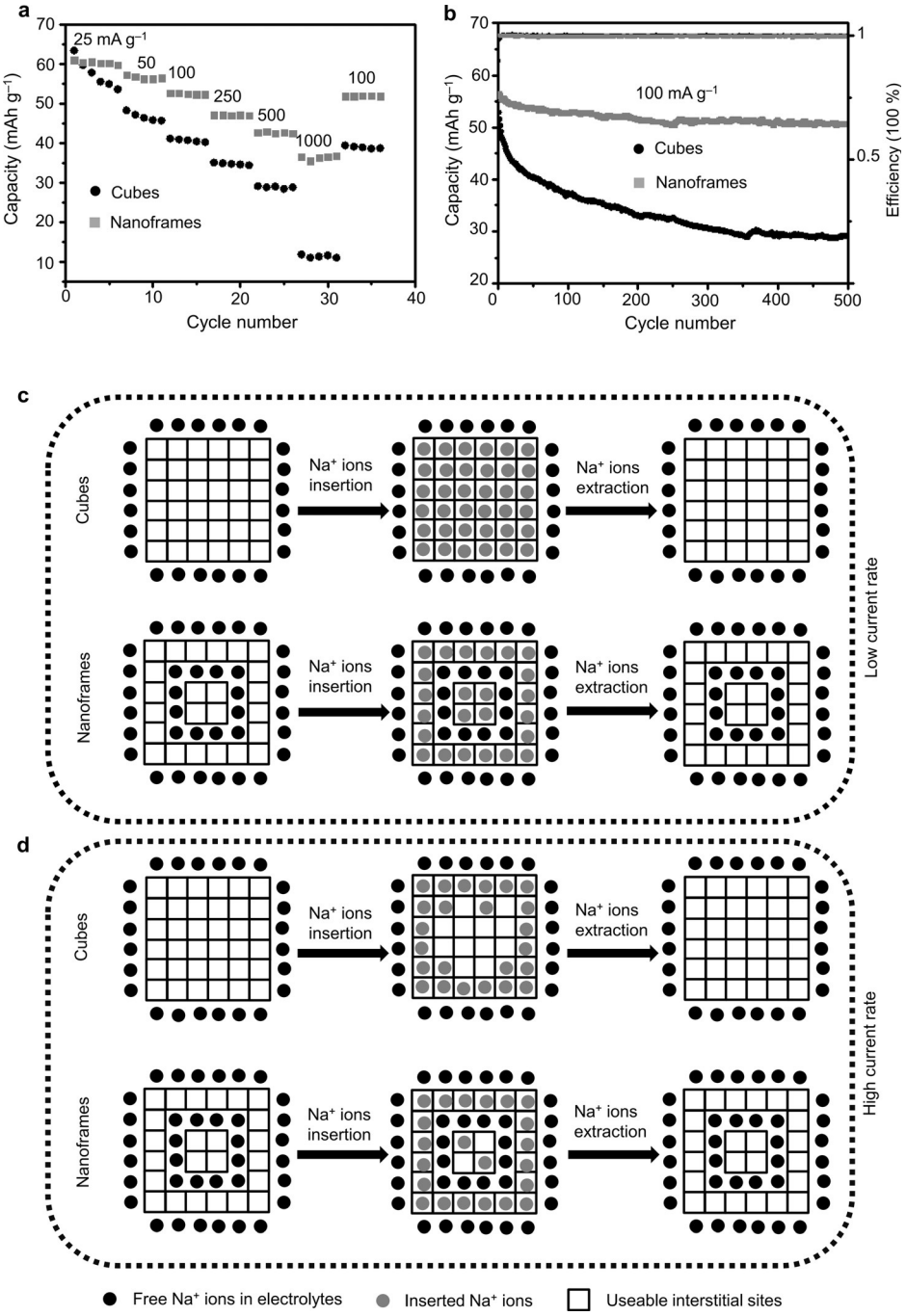

Figure 2. a) Rate performance of PBA as a cathode for a sodium ion battery. b) Cycling performance of PBA as a cathode for a sodium ion battery at a current rate of $100\ mA g^{-1}$. c) and d) The insertion/extraction of sodium ions into NiFe(II) PBA cubes and NiFe(II) PBA nanoframes at different current rates.

ure 2b). In the case of the initial cubes, only 55% of the initial capacity was maintained after 500 cycles. To clarify whether the enhanced rate performance and cycling stability of the nanoframes arises because of the *fcc* frameworks, we synthesized PBA cubic crystals with *fcc* frameworks (Supporting Information, Figures S10–S11). As a sodium ion battery cathode, the capacity of the cubes (*fcc*) was much lower than that of the nanoframes in terms of rate performance and cycling tests (Supporting Information, Figures S12–S13).

The crystal structure and shape of the PBA cubes are quite stable at various charge/discharge stages and after long term cycling, as suggested by Figures S14–S16 (Supporting Information). In the case of the nanoframes, the crystal structure and morphology are quite stable after electrochemical activation as well. No significant change was found at various charge/discharge stages, or after 500 cycles (Supporting Information, Figures S17–S19). As both the cubes and nanoframes are quite stable, the better rate performance and cycling stability of the nanoframes showcase the potential of the nanoframe structure. Elemental mapping was used to determine the distribution of sodium inside the initial cubes and nanoframes after insertion of Na^+ ions at a high current rate (1000 mA g^{-1}). Figure S20a (Supporting Information) shows that the distribution of Na^+ ions in the center is less than that at the surface of the initial cubes, suggesting that Na^+ ions are hardly transported into the cubes at a high current rate. However, high concentrations of Na^+ can be found even in the central part of the nanoframes after insertion of Na^+ ions at a high current rate (1000 mA g^{-1}; Supporting Information, Figure S20b).

A likely mechanism was proposed on the basis of the results, as shown in Figure 2c,d. To utilize all of the interstitial sites available in the cubes, Na^+ ions are required to travel from the surface into the center. Whereas in the nanoframes, Na^+ ions must diffuse through a much shorter path so as to occupy all the interstitial sites inside the skeleton. At a low current rate (Figure 2c), Na^+ ions are almost fully inserted into and extracted from both the cubes and nanoframes during the initial cycles. When the current rate increases (>100 mA g^{-1}), Na^+ ions are prevented from accessing the central part of the cubes during the insertion process, whereas a large percentage of the interstitial sites of the nanoframes may be accessed (Figure 2d; Supporting Information, Figure S20). Therefore, the nanoframes possess a much larger specific capacitance (especially at a high current rate >100 mA g^{-1}), indicative of an excellent rate-performance. Additionally, as our cycling tests were performed at a high current rate, the cycling stability of the nanoframes is superior to that of the cubes.

To further demonstrate the generality of the controlled etching concept, the lithium ion intercalation behaviors of the nanoframes and cubes were compared. Figure S21 (Supporting Information) illustrates that the nanoframes exhibit a much higher and more stable cycling capacitance than the initial cubes at a current rate of 200 mA g^{-1}. According to the charge/discharge curves (Supporting Information, Figures S22 and S23), Li^+ ions are able to intercalate in the nanoframes more easily than in the initial cubes, which agrees with the Na^+ ion intercalation experiments. These results demonstrate that the nanoframe structure helpfully enhances the high-rate and long-term intercalation of alkaline ions.

In summary, we have developed a method to synthesize monocrystalline PBA nanoframes by preferential etching. The heterogeneously distributed defects of the PBA crystals were essential to ensure selective etching at the surface face, rather than the corners or edges. The nanoframes retained monocrystalline frameworks after etching and improved the electrochemical performance of PBAs significantly. Excellent rate performances at high current rates were recorded when the nanoframes were used as a cathode. Moreover, cycling stability was obtained at high current rate after long-term charge/discharge cycles. This work highlights the utility of etching for the micro-fabrication of PBAs. PBA nanoframes offer major advantages in application-based roles because of their high surface-to-volume ratio, good crystallinity, and 3D contactable surface.

Acknowledgements

This work was supported by the National Natural Science Foundation of China (grant no. 21401056, 21173084, and 21473059) and Large Instruments Open Foundation of East China Normal University.

Keywords: alkali metals · coordination compounds · hollow nanostructures · ion insertion/extraction · surface etching

How to cite: *Angew. Chem. Int. Ed.* **2016**, *55*, 8228–8234
Angew. Chem. **2016**, *128*, 8368–8374

[1] a) A. G. Wong-Foy, A. J. Matzger, O. M. Yaghi, *J. Am. Chem. Soc.* **2006**, *128*, 3494–3495; b) M. Eddaoudi, J. Kim, N. Rosi, D. Vodak, J. Wachter, M. O'Keeffe, O. M. Yaghi, *Science* **2002**, *295*, 469–472; c) C. Serre, F. Millange, C. Thouvenot, M. Nogues, G. Marsolier, D. Louer, G. Ferey, *J. Am. Chem. Soc.* **2002**, *124*, 13519–13526; d) C. M. Doherty, G. Grenci, R. Ricco, J. I. Mardel, J. Reboul, S. Furukawa, S. Kitagawa, A. J. Hill, P. Falcaro, *Adv. Mater.* **2013**, *25*, 4701–4705; e) P. Falcaro, S. Furukawa, *Angew. Chem. Int. Ed.* **2012**, *51*, 8431–8433; *Angew. Chem.* **2012**, *124*, 8557–8559; f) P. Falcaro, R. Ricco, C. M. Doherty, K. Liang, A. J. Hill, M. J. Styles, *Chem. Soc. Rev.* **2014**, *43*, 5513–5560; g) K. Liang, R. Ricco, C. M. Doherty, M. J. Styles, S. Bell, N. Kirby, S. Mudie, D. Haylock, A. J. Hill, C. J. Doonan, P. Falcaro, *Nat. Commun.* **2015**, *6*, 7240; h) S. Furukawa, J. Reboul, S. Diring, K. Sumida, S. Kitagawa, *Chem. Soc. Rev.* **2014**, *43*, 5700–5734; i) K. Hirai, J. Reboul, N. Morone, J. E. Heuser, S. Furukawa, S. Kitagawa, *J. Am. Chem. Soc.* **2014**, *136*, 14966–14973; j) K. Sumida, N. Moitra, J. Reboul, S. Fukumoto, K. Nakanishi, K. Kanamori, S. Furukawa, S. Kitagawa, *Chem. Sci.* **2015**, *6*, 5938–5946; k) K. Sumida, D. L. Rogow, J. A. Mason, T. M. McDonald, E. D. Bloch, Z. R. Herm, T.-H. Bae, J. R. Long, *Chem. Rev.* **2012**, *112*, 724–781; l) K. Sumida, M. R. Hill, S. Horike, A. Dailly, J. R. Long, *J. Am. Chem. Soc.* **2009**, *131*, 15120–15121; m) V. Malgras, Q. Ji, Y. Kamachi, T. Mori, F.-K. Shieh, K. C. W. Wu, K. Ariga, Y. Yamauchi, *Bull. Chem. Soc. Jpn.* **2015**, *88*, 1171–1200.

[2] a) S.-L. Li, Q. Xu, *Energy Environ. Sci.* **2013**, *6*, 1656–1683; b) D. Wu, Z. Guo, X. Yin, Q. Pang, B. Tu, L. Zhang, Y.-G. Wang, Q. Li, *Adv. Mater.* **2014**, *26*, 3258–3262; c) G. Férey, F. Millange, M. Morcrette, C. Serre, M.-L. Doublet, J.-M. Grenèche, J.-M. Tarascon, *Angew. Chem. Int. Ed.* **2007**, *46*, 3259–3263; *Angew.*

Chem. **2007**, *119*, 3323 – 3327; d) S. Maiti, A. Pramanik, U. Manju, S. Mahanty, *ACS Appl. Mater. Interfaces* **2015**, *7*, 16357 – 16363; e) G. de Combarieu, M. Morcrette, F. Millange, N. Guillou, J. Cabana, C. P. Grey, I. Margiolaki, G. Ferey, J. M. Tarascon, *Chem. Mater.* **2009**, *21*, 1602 – 1611; f) Z. Ma, Y. Wang, C. Sun, J. A. Alonso, M. T. Fernandez-Diaz, L. Chen, *Sci. Rep.* **2014**, *4*, 7231.

[3] a) K. M. Choi, H. M. Jeong, J. H. Park, Y.-B. Zhang, J. K. Kang, O. M. Yaghi, *ACS Nano* **2014**, *8*, 7451 – 7457; b) L. Wang, X. Feng, L. Ren, Q. Piao, J. Zhong, Y. Wang, H. Li, Y. Chen, B. Wang, *J. Am. Chem. Soc.* **2015**, *137*, 4920 – 4923; c) N. Campagnol, R. Romero-Vara, W. Deleu, L. Stappers, K. Binnemans, D. E. De Vos, J. Fransaer, *ChemElectroChem* **2014**, *1*, 1182 – 1188.

[4] a) Y. You, X.-L. Wu, Y.-X. Yin, Y.-G. Guo, *Energy Environ. Sci.* **2014**, *7*, 1643 – 1647; b) X. Wu, W. Deng, J. Qian, Y. Cao, X. Ai, H. Yang, *J. Mater. Chem. A* **2013**, *1*, 10130 – 10134; c) M. Takachi, T. Matsuda, Y. Moritomo, *Jpn. J. Appl. Phys.* **2013**, *52*, 044301; d) Y. Moritomo, K. Wakaume, M. Takachi, X. Zhu, H. Kamioka, *J. Phys. Soc. Jpn.* **2013**, *82*, 094710; e) T. Matsuda, M. Takachi, Y. Moritomo, *Chem. Commun.* **2013**, *49*, 2750 – 2752; f) M. Okubo, C. H. Li, D. R. Talham, *Chem. Commun.* **2014**, *50*, 1353 – 1355; g) D. Asakura, C. H. Li, Y. Mizuno, M. Okubo, H. Zhou, D. R. Talham, *J. Am. Chem. Soc.* **2013**, *135*, 2793 – 2799; h) S. Kajiyama, Y. Mizuno, M. Okubo, R. Kurono, S.-i. Nishimura, A. Yamada, *Inorg. Chem.* **2014**, *53*, 3141 – 3147; i) Y. Mizuno, M. Okubo, E. Hosono, T. Kudo, H. Zhou, K. Oh-ishi, *J. Phys. Chem. C* **2013**, *117*, 10877 – 10882; j) M. Okubo, K. Kagesawa, Y. Mizuno, D. Asakura, E. Hosono, T. Kudo, H. Zhou, K. Fujii, H. Uekusa, S.-i. Nishimura, A. Yamada, A. Okazawa, N. Kojima, *Inorg. Chem.* **2013**, *52*, 3772 – 3779.

[5] Y. Yue, A. J. Binder, B. Guo, Z. Zhang, Z.-A. Qiao, C. Tian, S. Dai, *Angew. Chem. Int. Ed.* **2014**, *53*, 3134 – 3137; *Angew. Chem.* **2014**, *126*, 3198 – 3201.

[6] a) M. A. Mahmoud, W. Qian, M. A. El-Sayed, *Nano Lett.* **2011**, *11*, 3285 – 3289; b) C. Chen, Y. Kang, Z. Huo, Z. Zhu, W. Huang, H. L. Xin, J. D. Snyder, D. Li, J. A. Herron, M. Mavrikakis, M. Chi, K. L. More, Y. Li, N. M. Markovic, G. A. Somorjai, P. Yang, V. R. Stamenkovic, *Science* **2014**, *343*, 1339 – 1343; c) B. Y. Xia, H. B. Wu, X. Wang, X. W. Lou, *Angew. Chem. Int. Ed.* **2013**, *52*, 12337 – 12340; *Angew. Chem.* **2013**, *125*, 12563 – 12566; d) X. Shuifen, L. Ning, X. Zhaoxiong, W. Jinguo, M. J. Kim, X. Younan, *Angew. Chem. Int. Ed.* **2012**, *51*, 10266 – 10270; *Angew. Chem.* **2012**, *124*, 10412 – 10416; e) L.-I. Hung, C.-K. Tsung, W. Huang, P. Yang, *Adv. Mater.* **2010**, *22*, 1910 – 1914; f) Z. Wang, D. Luan, F. Y. C. Boey, X. W. Lou, *J. Am. Chem. Soc.* **2011**, *133*, 4738 – 4741; g) X.-Y. Yu, L. Yu, H. B. Wu, X. W. Lou, *Angew. Chem. Int. Ed.* **2015**, *54*, 5331 – 5335; *Angew. Chem.* **2015**, *127*, 5421 – 5425; h) Y. Wu, D. Wang, G. Zhou, R. Yu, C. Chen, Y. Li, *J. Am. Chem. Soc.* **2014**, *136*, 11594 – 11597; i) D. Kim, J. Park, K. An, N.-K. Yang, J.-G. Park, T. Hyeon, *J. Am. Chem. Soc.* **2007**, *129*, 5812 – 5813.

[7] a) F. Zhang, Y. Wei, X. Wu, H. Jiang, W. Wang, H. Li, *J. Am. Chem. Soc.* **2014**, *136*, 13963 – 13966; b) H. J. Lee, W. Cho, M. Oh, *Chem. Commun.* **2012**, *48*, 221 – 223; c) Y. Yang, F. Wang, Q. Yang, Y. Hu, H. Yan, Y.-Z. Chen, H. Liu, G. Zhang, J. Lu, H.-L. Jiang, H. Xu, *ACS Appl. Mater. Interfaces* **2014**, *6*, 18163 – 18171; d) J. Yang, F. Zhang, H. Lu, X. Hong, H. Jiang, Y. Wu, Y. Li, *Angew. Chem. Int. Ed.* **2015**, *54*, 10889 – 10893; *Angew. Chem.* **2015**, *127*, 11039 – 11043.

[8] a) R. Ameloot, F. Vermoortele, W. Vanhove, M. B. J. Roeffaers, B. F. Sels, D. E. De Vos, *Nat. Chem.* **2011**, *3*, 382 – 387; b) A. J. Brown, N. A. Brunelli, K. Eum, F. Rashidi, J. R. Johnson, W. J. Koros, C. W. Jones, S. Nair, *Science* **2014**, *345*, 72 – 75; c) A. Carné-Sánchez, I. Imaz, M. Cano-Sarabia, D. Maspoch, *Nat. Chem.* **2013**, *5*, 203 – 211; d) J. Huo, L. Wang, E. Irran, H. Yu, J. Gao, D. Fan, B. Li, J. Wang, W. Ding, A. M. Amin, C. Li, L. Ma, *Angew. Chem. Int. Ed.* **2010**, *49*, 9237 – 9241; *Angew. Chem.* **2010**, *122*, 9423 – 9427; e) H. Kim, M. Oh, D. Kim, J. Park, J. Seong, S. K. Kwak, M. S. Lah, *Chem. Commun.* **2015**, *51*, 3678 – 3681; f) T. Palaniselvam, B. P. Biswal, R. Banerjee, S. Kurungot, *Chem. Eur. J.* **2013**, *19*, 9335 – 9342; g) M. Pang, A. J. Cairns, Y. Liu, Y. Belmabkhout, H. C. Zeng, M. Eddaoudi, *J. Am. Chem. Soc.* **2013**, *135*, 10234 – 10237; h) X. Roy, J. K. H. Hui, M. Rabnawaz, G. Liu, M. J. MacLachlan, *J. Am. Chem. Soc.* **2011**, *133*, 8420 – 8423; i) Z. Zhang, Y. Chen, X. Xu, J. Zhang, G. Xiang, W. He, X. Wang, *Angew. Chem. Int. Ed.* **2014**, *53*, 429 – 433; *Angew. Chem.* **2014**, *126*, 439 – 443; j) K. Jayaramulu, K. S. Krishna, S. J. George, M. Eswaramoorthy, T. K. Maji, *Chem. Commun.* **2013**, *49*, 3937 – 3939.

[9] a) M. Hu, S. Furukawa, R. Ohtani, H. Sukegawa, Y. Nemoto, J. Reboul, S. Kitagawa, Y. Yamauchi, *Angew. Chem. Int. Ed.* **2012**, *51*, 984 – 988; *Angew. Chem.* **2012**, *124*, 1008 – 1012; b) R. McHale, Y. Liu, N. Ghasdian, N. S. Hondow, S. Ye, Y. Lu, R. Brydson, X. Wang, *Nanoscale* **2011**, *3*, 3685 – 3694; c) Q. Shen, J. Jiang, M. Fan, S. Liu, L. Wang, Q. Fan, W. Huang, *J. Electroanal. Chem.* **2014**, *712*, 132 – 138; d) O. N. Risset, E. S. Knowles, S. Ma, M. W. Meisel, D. R. Talham, *Chem. Mater.* **2013**, *25*, 42 – 47.

[10] a) J. B. Joo, I. Lee, M. Dahl, G. D. Moon, F. Zaera, Y. Yin, *Adv. Funct. Mater.* **2013**, *23*, 4246 – 4254; b) Q. Zhang, I. Lee, J. Ge, F. Zaera, Y. Yin, *Adv. Funct. Mater.* **2010**, *20*, 2201 – 2214; c) Q. Zhang, T. Zhang, J. Ge, Y. Yin, *Nano Lett.* **2008**, *8*, 2867 – 2871.

[11] C. Avci, J. Arinez-Soriano, A. Carne-Sanchez, V. Guillerm, C. Carbonell, I. Imaz, D. Maspoch, *Angew. Chem. Int. Ed.* **2015**, *54*, 14417 – 14421; *Angew. Chem.* **2015**, *127*, 14625 – 14629.

[12] a) H. Furukawa, U. Mueller, O. M. Yaghi, *Angew. Chem. Int. Ed.* **2015**, *54*, 3417 – 3430; *Angew. Chem.* **2015**, *127*, 3480 – 3494; b) M. Hu, A. A. Belik, M. Imura, Y. Yamauchi, *J. Am. Chem. Soc.* **2013**, *135*, 384 – 391; c) Z. Fang, J. P. Duerholt, M. Kauer, W. Zhang, C. Lochenie, B. Jee, B. Albada, N. Metzler-Nolte, A. Poeppl, B. Weber, M. Muhler, Y. Wang, R. Schmid, R. A. Fischer, *J. Am. Chem. Soc.* **2014**, *136*, 9627 – 9636; d) O. Kozachuk, I. Luz, F. X. Llabres i Xamena, H. Noei, M. Kauer, H. B. Albada, E. D. Bloch, B. Marler, Y. Wang, M. Muhler, R. A. Fischer, *Angew. Chem. Int. Ed.* **2014**, *53*, 7058 – 7062; *Angew. Chem.* **2014**, *126*, 7178 – 7182; e) B. Tu, Q. Pang, D. Wu, Y. Song, L. Weng, Q. Li, *J. Am. Chem. Soc.* **2014**, *136*, 14465 – 14471.

[13] a) L. Wang, J. Song, R. Qiao, L. A. Wray, M. A. Hossain, Y.-D. Chuang, W. Yang, Y. Lu, D. Evans, J.-J. Lee, S. Vail, X. Zhao, M. Nishijima, S. Kakimoto, J. B. Goodenough, *J. Am. Chem. Soc.* **2015**, *137*, 2548 – 2554; b) J. Song, L. Wang, Y. Lu, J. Liu, B. Guo, P. Xiao, J.-J. Lee, X.-Q. Yang, G. Henkelman, J. B. Goodenough, *J. Am. Chem. Soc.* **2015**, *137*, 2658 – 2664; c) Y. Liu, Y. Qiao, W. Zhang, Z. Li, X. Ji, L. Miao, L. Yuan, X. Hu, Y. Huang, *Nano Energy* **2015**, *12*, 386 – 393; d) Y. You, X. Yu, Y. Yin, K.-W. Nam, Y.-G. Guo, *Nano Res.* **2015**, *8*, 117 – 128; e) W.-J. Li, S.-L. Chou, J.-Z. Wang, Y.-M. Kang, J.-L. Wang, Y. Liu, Q.-F. Gu, H.-K. Liu, S.-X. Dou, *Chem. Mater.* **2015**, *27*, 1997 – 2003; f) L. Shen, Z. Wang, L. Chen, *Chem. Eur. J.* **2014**, *20*, 12559 – 12562; g) S. Yu, Y. Li, Y. Lu, B. Xu, Q. Wang, M. Yan, Y. Jiang, *J. Power Sources* **2015**, *275*, 45 – 49; h) W.-J. Li, S.-L. Chou, J.-Z. Wang, J.-L. Wang, Q.-F. Gu, H.-K. Liu, S.-X. Dou, *Nano Energy* **2015**, *13*, 200 – 207; i) D. Yang, J. Xu, X.-Z. Liao, H. Wang, Y.-S. He, Z.-F. Ma, *Chem. Commun.* **2015**, *51*, 8181 – 8184; j) X. Wu, Y. Luo, M. Sun, J. Qian, Y. Cao, X. Ai, H. Yang, *Nano Energy* **2015**, *13*, 117 – 123; k) C. D. Wessells, S. V. Peddada, R. A. Huggins, Y. Cui, *Nano Lett.* **2011**, *11*, 5421 – 5425; l) C. D. Wessells, R. A. Huggins, Y. Cui, *Nat. Commun.* **2011**, *2*, 550.

[14] Y.-D. Chiang, M. Hu, Y. Kamachi, S. Ishihara, K. Takai, Y. Tsujimoto, K. Ariga, K. C. W. Wu, Y. Yamauchi, *Eur. J. Inorg. Chem.* **2013**, 3141 – 3145.

[15] M. Hu, J. S. Jiang, *Mater. Res. Bull.* **2011**, *46*, 702 – 707.

[16] D. Yang, X.-Z. Liao, B. Huang, J. Shen, Y.-S. He, Z.-F. Ma, *J. Mater. Chem. A* **2013**, *1*, 13417 – 13421.

[17] K. M. Jeerage, W. A. Steen, D. T. Schwartz, *Langmuir* **2002**, *18*, 3620 – 3625.
[18] P. J. Kulesza, M. A. Malik, A. Denca, J. Strojek, *Anal. Chem.* **1996**, *68*, 2442 – 2446.
[19] L. Wang, Y. Lu, J. Liu, M. Xu, J. Cheng, D. Zhang, J. B. Goodenough, *Angew. Chem. Int. Ed.* **2013**, *52*, 1964 – 1967; *Angew. Chem.* **2013**, *125*, 2018 – 2021.
[20] a) Y. Cao, L. Xiao, M. L. Sushko, W. Wang, B. Schwenzer, J. Xiao, Z. Nie, L. V. Saraf, Z. Yang, J. Liu, *Nano Lett.* **2012**, *12*, 3783 – 3787; b) Y. Cao, L. Xiao, W. Wang, D. Choi, Z. Nie, J. Yu, L. V. Saraf, Z. Yang, J. Liu, *Adv. Mater.* **2011**, *23*, 3155 – 3160; c) J. Qian, X. Wu, Y. Cao, X. Ai, H. Yang, *Angew. Chem. Int. Ed.* **2013**, *52*, 4633 – 4636; *Angew. Chem.* **2013**, *125*, 4731 – 4734; d) J. Qian, M. Zhou, Y. Cao, X. Ai, H. Yang, *Adv. Energy Mater.* **2012**, *2*, 410 – 414; e) B. Dunn, H. Kamath, J.-M. Tarascon, *Science* **2011**, *334*, 928 – 935; f) B. L. Ellis, W. R. M. Makahnouk, Y. Makimura, K. Toghill, L. F. Nazar, *Nat. Mater.* **2007**, *6*, 749 – 753; g) S.-W. Kim, D.-H. Seo, X. Ma, G. Ceder, K. Kang, *Adv. Energy Mater.* **2012**, *2*, 710 – 721; h) V. Palomares, P. Serras, I. Villaluenga, K. B. Hueso, J. Carretero-Gonzalez, T. Rojo, *Energy Environ. Sci.* **2012**, *5*, 5884 – 5901; i) H. Pan, Y.-S. Hu, L. Chen, *Energy Environ. Sci.* **2013**, *6*, 2338 – 2360; j) K. Tang, L. Fu, R. J. White, L. Yu, M.-M. Titirici, M. Antonietti, J. Maier, *Adv. Energy Mater.* **2012**, *2*, 873 – 877; k) H. Yu, Y. Ren, D. Xiao, S. Guo, Y. Zhu, Y. Qian, L. Gu, H. Zhou, *Angew. Chem. Int. Ed.* **2014**, *53*, 8963 – 8969; *Angew. Chem.* **2014**, *126*, 9109 – 9115; l) B. Jache, P. Adelhelm, *Angew. Chem. Int. Ed.* **2014**, *53*, 10169 – 10173; *Angew. Chem.* **2014**, *126*, 10333 – 10337; m) C. Bommier, T. W. Surta, M. Dolgos, X. Ji, *Nano Lett.* **2015**, *15*, 5888 – 5892; n) Z. Jian, W. Luo, X. Ji, *J. Am. Chem. Soc.* **2015**, *137*, 11566 – 11569; o) W. Luo, J. Schardt, C. Bommier, B. Wang, J. Razink, J. Simonsen, X. Ji, *J. Mater. Chem. A* **2013**, *1*, 10662 – 10666.

Received: January 20, 2016
Revised: March 24, 2016
Published online: June 29, 2016

